Potential of Near-infrared Spectroscopy to Detect Defects on the Surface of Solid Wood Boards

Jun Cao,[a] Hao Liang,[a] Xue Lin,[b] Wenjun Tu,[a] and Yizhuo Zhang [a,*]

Defects on the surface of solid wood boards directly affect their mechanical properties and product grades. This study investigated the use of near-infrared spectroscopy (NIRS) to detect and classify defects on the surface of solid wood boards. *Pinus koraiensis* was selected as the raw material. The experiments focused on the ability to use the model to sort defects on the surface of wood into four types, namely live knots, dead knots, cracks, and defect-free. The test data consisted of 360 NIR absorption spectra of the defect samples using a portable NIR spectrometer, with the wavelength range of 900 to 1900 nm. Three pre-processing methods were used to compare the effects of noise elimination in the original absorption spectra. The NIR discrimination models were developed based on partial least squares and discriminant analysis (PLS-DA), least squares support vector machine (LS-SVM), and back-propagation neural network (BPNN) from 900 to approximately 1900 nm. The results demonstrated that the BPNN model exhibited the highest classification accuracy of 97.92% for the model calibration and 97.50% for the prediction set. These results suggest that there is potential for the NIR method to detect defects and differentiate between types of defects on the surface of solid wood boards.

Keywords: Surface defects; Solid wood boards; Near-infrared spectroscopy; PLS - DA; BPNN; LS-SVM

*Contact information: a: College of Mechanical and Electrical Engineering, Northeast Forestry University, Harbin, 150040, China; b: Material Science and Engineering College, Northeast Forestry University, Harbin, 150040, China; *Corresponding authors: nefuzyz@163.com*

INTRODUCTION

Wood is a very important construction material that can achieve a high degree of structural performance and reliability. In recent years researchers have studied various aspects of wood to evaluate its quality and grade. Solid wood boards play a key role in the performance of building decoration. Therefore, the detection of surface defect information has become a necessary part of solid wood processing. Because of the complexity of the texture and color of wood, it is difficult for visual methods to detect the surface defects of boards correctly, especially those that are small in size. Therefore, a fast and accurate method of detection is needed to determine and classify the surface defects on solid wood boards.

In recent years, several new wood surface defect detection techniques have arisen, including ultrasonic technology (Kabir *et al.* 2003), microwave technology (Baradit *et al.* 2006), and X-rays (Cristhian *et al.* 2008). However, the detection of defects on the surface of solid wood boards needs to be rapid, inexpensive, and simple to operate and industrialize. Near-infrared (NIR) spectroscopy can meet these requirements and is contactless, nondestructive, and free of radiation hazards.

As a nondestructive detection technology, NIR spectroscopy has been applied for several uses in wood research, for example, wood color (Yang *et al.* 2012), basic density (Santos *et al.* 2012), moisture content (Eom *et al.* 2013), drying stress level (Ken *et al.* 2013), and surface roughness (Zhang *et al.* 2015). In addition, NIR spectroscopy has also been used to detect defects on the surface of veneers according to size (Yang *et al.* 2016). All of these implementations show that NIR spectroscopy is a feasible tool to measure the properties of wood.

To detect and classify defects on the surface of solid wood boards, this study chose the derivative approach combined with Savitzky-Golay as the pre-processing method by analyzing the results of various pre-processing methods for the original NIR data using partial least squares regression (PLSR) and principal component regression (PCR) models. Additionally, the study selected three models, partial least squares and discriminant analysis (PLS-DA), least squares support vector machines (LS-SVM), and back propagation neural network (BPNN), to detect and classify the types of defects on the surface of solid wood boards. The predictive effects and classification of the different models were compared, and the BPNN model yielded the best results for defect classification. The main purpose of this study was to investigate the ability of NIR spectroscopy to detect defects on the surface of solid wood boards, to compare the effects of various pre-processing methods on original NIR absorption data, to develop calibrations for detecting defects on the surface of solid wood boards using NIR spectroscopy, and to evaluate the predictive and classification ability of the calibrations.

EXPERIMENTAL

Specimen Preparation

Pinus koraiensis, known as Korean pine, is a very good material for furniture making. Wood was obtained from a forest in the northeast of China (128°53’ 20” and 47°10’ 50”). The logs were cut at a height of 1.5 m and then were air-dried. After air-drying, all logs were cut into small boards of 400 mm x 200 mm x 20 mm. In accordance with national standards, “Defects in sawn timber (GB/T 4823-2013)”, the boards with different types of surface defects were accordingly selected and divided into four categories (live knots, dead knots, cracks, and defect-free). A total of 360 samples with four kinds of surface defects were prepared (Table 1). The samples were randomly allocated to two groups: 240 samples for the calibration set and 120 samples for the prediction set.

Table 1. Statistics of the Defects Types from the Calibration and Prediction Sets

Defect types	Number of samples		
	Calibration set	Prediction set	Total
Live Knots	60	30	90
Dead Knots	60	30	90
Cracks	60	30	90
Defect-free	60	30	90
All	240	120	360

Table 2. Statistics of the Defects Types from the Calibration and Prediction Sets

Defect types	Number of samples		
	Calibration set	Prediction set	Total
Live Knots	60	30	90
Dead Knots	60	30	90
Cracks	60	30	90
Defect-free	60	30	90
All	240	120	360

NIR Spectra Measurements

The NIR absorption spectra were acquired using an ultra-compact NIR fiber optic spectrometer (Insion Co., Gmbh, Heilbronn, Germany) from 900 to 1900 nm at a resolution of 9 nm. The spectrometer had two fiber optic probes to scan the sample surface. These were oriented at an angle of 90° above the surface of the solid wood boards. The NIR spectra data were collected using SPEC view 7.1 software (Insion Co., GmbH, Heilbronn, Germany) and exported as Excel (Microsoft, Redmond, WA) files. All measurements were taken under laboratory conditions, 20 ± 2 °C and 40% to 50% relative humidity. Thirty spectra from each sample were collected and then averaged to a single spectrum to represent a pooled mean. The wavelengths from 1000 to 1600 nm contained the majority of the information about the wood properties (Todorović *et al.* 2015).

Pre-Processing of NIR Spectra

Pre-processing is necessary and important to eliminate high-frequency noise, baseline drift, light scattering, and other negative effects in the spectra and to subsequently improve the regression, classification model, or exploratory analysis. There are many pre-processing methods, including normalization, smoothing, and Fourier transform. Multiplicative scatter correction (MSC) and standard normal variate (SNV) calculation were used to accomplish scatter correction and also to adjust the baseline excursion (Rinnan *et al.* 2009). Derivative combined with Savitzky-Golay was capable of effectively removing the interference of baseline and other backgrounds, resolving overlapping peaks, and improving resolution and sensitivity. In addition, Savitzky-Golay derivation smoothed the raw data. Data were pre-processed using the MSC and SNV, as well as taking the derivative combined with Savitzky-Golay (derivative combined with Savitzky-Golay polynomial order = 2, smoothing point = 5).

Statistical Analysis

Partial least squares (PLS)

PLS investigates relationships between spectral and concentration data. The PLS model was fit using the non-linear iterative partial least squares (NIPALS) algorithm with the cross-validation of eight randomly chosen segments. The latent variables of PLS were selected to relate to the set of responses to optimize the latent variables' ability to describe the variance in responses and to improve predictability. PLS can be used for both the data classification and prediction of responses (Danvind 2002).

Partial least squares and discriminant analysis (PLS-DA)

PLS-DA is a variant of PLS. In this method, PLS-DA is performed to build models for classification. The models were developed and cross-validated for an optimum number of components using partial least squares regression and setting different values for different types of surface defects (Takizawa *et al.* 2014). The ideal values predicted by PLS-DA are integers, but in practice, these values only approximate these numbers. It was assumed that the predicted *y* values followed a distribution similar to what will be observed for future samples. With these estimated distributions, a threshold was calculated to optimize a model for future predictions (Nascimbem *et al.* 2013).

Least squares support vector machines (LS-SVM)

Least squares support vector machine (LS-SVM) regression is a statistical learning method with a good theoretical foundation. It is an interesting renovation of SVM regression proposed by Suykens *et al.* (2002). LS-SVM is a nonlinear multivariate calibration method that adopts a least squares linear system as a loss function. LS-SVM has the capability for linear and non-linear multivariate calibration and quickly solving multivariate calibration problems (Li *et al.* 2016).

Back propagation neural network (BPNN)

Back propagation neural network (BPNN), a feed-forward network, is one of the most widely used neural networks. It uses a learning process to minimize the global error of the system by modifying node weights. The network is trained by initially selecting the weights at random and then presenting all training data repeatedly. The weights are then adjusted after every trial using external information to specify the correct result until the weights converge and the errors are reduced to acceptable values (Zhu *et al.* 2016). The neural network used in this study was established and consisted of an input layer, one or more hidden layers, and one output layer. Input data was obtained as the pre-processed absorbance spectra. The output neurons were using dummy variable values (1000 for live knots, 0100 for dead knots, 0010 for cracks, and 0001 for defect-free).

Chemometrics Software

The data import, pre-processing (MSC, SNV, derivative combined with Savitzky-Golay), and construction of classification models (PLS-DA, LS-SVM, and BPNN) were implemented in MATLAB R2012b software (Mathworks Inc, Natick, MA).

RESULTS AND DISCUSSION

Effects of Pre-Processing Spectra

Figure 1 shows the NIR absorption of all the defect-free samples from 900 to 1864 nm. It could be seen that the distribution range of the calibration set was larger than the prediction set. Such sets were employed so that the samples of the calibration set could be regarded as representative. It was possible to verify some high-frequency noise, baseline drift, and other negative effects from Fig. 1. Therefore, three pre-processing methods, MSC, SNV, and derivative combined with Savitzky-Golay, were performed with the raw data. To compare the effects of the pre-processing methods, PLSR and PCR were used to interpret the relationship between the calibration set and the prediction set. The performance of regression models was assessed using four statistical metrics: (1)

coefficient of determination of the calibration model (Rc^2); (2) coefficient of determination of the prediction model (Rp^2); (3) the root mean square error of calibration (RMSEC); and (4) the root mean square error of prediction (RMSEP). Table 2 shows the prediction results based on different models and pre-processing methods. The results of the models with different pre-processing methods are represented with R_c^2 values ranging between 0.925 and 0.994 and R_p^2 values ranging between 0.921 and 0.991.

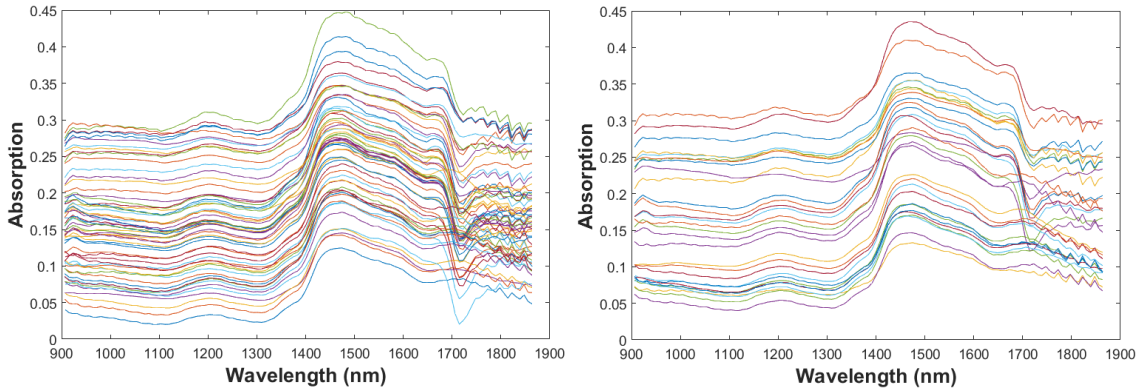

Fig. 1. Original spectra of the defect-free samples in the (a) calibration sets and (b) prediction sets.

Table 2. Prediction Results Based on Various Models and Pre-Processing Methods

Pre-Processing method		Unprocessed	MSC	SNV	DSG
PLSR	R_C^2	0.927	0.936	0.986	0.994
	RMSEC	0.04347	0.00943	0.00152	0.00034
	R_P^2	0.922	0.930	0.986	0.991
	RMSEP	0.04574	0.00946	0.00163	0.00037
PCR	R_C^2	0.926	0.928	0.975	0.983
	RMSEC	0.4369	0.00940	0.00255	0.00044
	R_P^2	0.921	0.925	0.976	0.984
	RMSEP	0.04562	0.00944	0.00253	0.00042

* PLSR: partial least squares; PCR: principal component regression; R_c^2: coefficient of determination of the calibration model; R_p^2: coefficient of determination of the prediction model; RMSEC: the root mean square error of calibration; RMSEP: the root mean square error of prediction; MSC: multiplicative scatter correction; SNV: standard normal variate; DSG: derivative combined with Savitzky-Golay

For the prediction models, the spectra pre-processed with the combination of derivative and Savitzky-Golay exhibited the best results with an R_c^2 of 0.994, RMSEC of 0.00034, R_p^2 of 0.991, and RMSEP of 0.00037 in PLSR model. Likewise, for the PCR model, the best results were provided by the combination of derivative and Savitzky-Golay, with an R_c^2 of 0.983, RMSEC 0.00044, R_p^2 of 0.984, and RMSEP of 0.00042. Figure 2 shows the wood spectra of samples that were pre-processed with the combination of derivative and Savitzky-Golay. The spectra were smoother and the noise and baseline drift were mostly eliminated. Figure 3 shows the mean spectra of various types of defects including live knots, dead knots, cracks, and defect-free after pre-processing. The spectra of four types of defects have some differences in the spectral range, especially in the range of 1468.16 to 1864 nm.

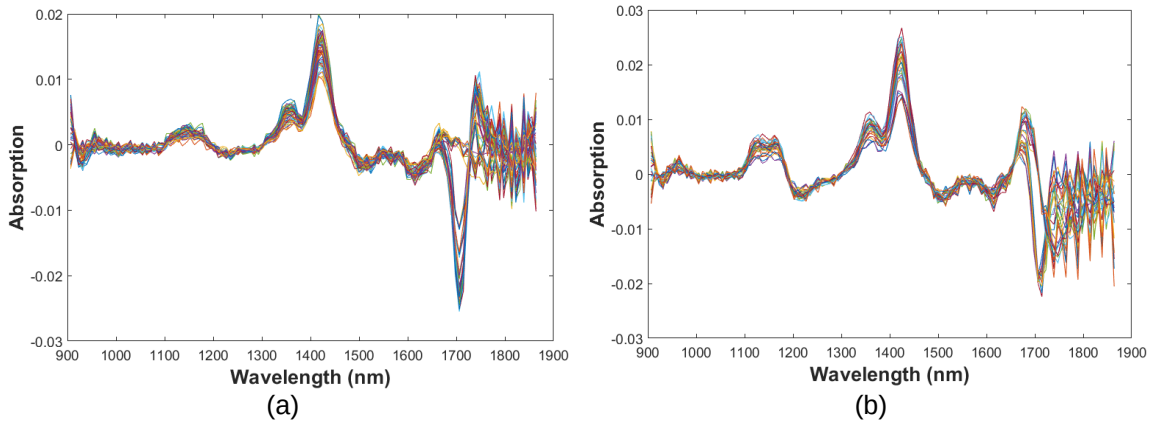

Fig. 2. Spectra of the defect-free samples pre-processed with a combination of derivative and Savitzky-Golay; (a) calibration sets; (b) prediction sets

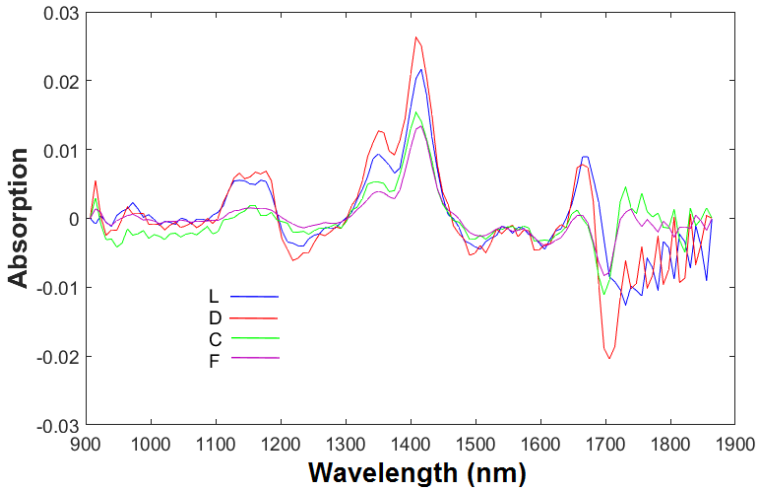

Fig. 3. NIR mean spectra of samples from different types of defects after pre-processing: L: live knots, D: dead knots, C: cracks, F: defect-free

Classification Results Based on Different Methods

The analytical performance for the classification of the types of defects was compared with the use of the linear regression method PLS-DA and the nonlinear regression methods LS-SVM and BP-ANN. All the methods were used to detect and discriminate defect types from the entire pool of defects.

Results using PLS-DA for different types of defects

First, the variable values of the calibration set were given according to the class feature of samples (Table 3). Table 4 shows the classification results for samples with different types of defects using the PLS-DA method. Four different types of defects were implemented in the model. It can be found that the average accuracy rates of the PLS-DA classification model for the calibration and prediction set were 90.00% and 86.67%, respectively; the overall accuracy rates of the PLS-DA model in identifying the defect-free samples of the calibration and prediction set were 98.33% and 96.67%, respectively; however, all the accuracies of samples with defects were less than 89.00%. It can be concluded that the ability of the PLS-DA model to discriminate the defect-free samples from the defected samples is feasible.

Table 3. Category Variables for Four Types of Defects using PLS-DA

Type of Defect	Variable Values
Live knots	[1 0]
Dead knots	[0 1]
Cracks	[1 1]
Defect-free	[0 0]

Table 4. Classification Results for Four Types of Defects

Type of Defect	Calibration Set		Prediction Set	
	Correct number	Classification accuracy (%)	Correct number	Classification accuracy (%)
Live knots	53	88.33	26	86.67
Dead knots	52	86.67	24	80.00
Cracks	52	86.67	25	83.33
Defect-free	59	98.33	29	96.67
Average	54	90.00	26	86.67

Results using LS-SVM for different types of defects

The discrimination results are shown in Table 5. The LS-SVM model identified 94.58% of the calibration samples correctly. For all samples in the prediction set, a prediction accuracy of 93.33% was obtained. Compared with the PLS-DA model, the performance of the LS-SVM model was better. The experiments suggested that the LS-SVM model could be used to classify the samples with the mentioned types of defects (live knots, dead knots, cracks, and defect-free).

Table 5. Classification Results for Four Types of Defects using LS-SVM

Type of Defect	Calibration Set					Prediction Set				
	Live knots	Dead knots	Cracks	Defect-free	Accuracy (%)	Live knots	Dead knots	Cracks	Defect-free	Accuracy (%)
Live knots	57	1	1	1	95	27	1	0	2	90
Dead knots	1	55	2	1	91.67	1	27	2	0	90
Cracks	1	2	56	1	93.33	1	1	28	0	93.33
Defect-free	1	0	0	59	98.33	0	0	0	30	100
Overall accuracy (%)	94.58					93.33				

Results using BPNN for different types of defects

In building the BPNN model, the minimum learning rate was set at 0.1, while the threshold residual error and the training time were set at 0.0001 and 1200 s, respectively. The discrimination results based on BPNN are shown in Table 6. It was found that 97.92% of the samples in the calibration set were correctly identified, which was better than those obtained by both the PLS-DA model and LS-SVM model. Likewise, 97.50% of the samples in the prediction set were correctly differentiated. For the samples in the prediction

set, those from cracks and defect-free were correctly distinguished, but one sample in the live knots was identified incorrectly and two were identified incorrectly in the dead knots.

Table 6. Classification Results for Four Types of Defects using BPNN

Type of Defect	Calibration Set					Prediction Set				
	Live knots	Dead knots	Cracks	Defect-free	Accuracy (%)	Live knots	Dead knots	Cracks	Defect-free	Accuracy (%)
Live knots	59	0	0	1	98.33	29	0	0	1	96.67
Dead knots	1	57	2	0	95	1	28	1	0	93.33
Cracks	0	1	59	0	98.33	0	0	30	0	100
Defect-free	0	0	0	60	100	0	0	0	30	100
Overall accuracy (%)	97.92					97.50				

In comparison, the BPNN results were the best among the three models. Particularly, the identification rate of 97.50% for the prediction samples and the identification rate of 97.92% for the calibration samples were higher than that obtained by both the LS-SVM model and the PLS-DA model. These experiments showed that the BPNN model performed better and also demonstrated that NIR spectroscopy combined with BPNN and LS-SVM could be utilized to identify the defects on the surface of solid wood boards.

CONCLUSIONS

1. Compared with the prediction results based on various models and pre-processing methods, the combination of derivative and the Savitzky-Golay algorithm was most capable of pre-processing the original spectra of the samples.
2. Three pattern recognition methods, PLS-DA, BPNN, and LS-SVM, were used to build a model for the differentiation of defects on the surface of the solid wood board. The results indicated that the BPNN model performed better than both PLS-DA and LS-SVM, as shown by its respective classification accuracy. The classification accuracies were 97.92% and 97.50% for the calibration set and the prediction set, respectively.
3. This research demonstrated that NIR spectroscopy in combination with BPNN and LS-SVM has the potential to detect and classify the different types of defects on the surface of the solid wood boards and offered a new approach to quickly distinguishing the defects. While PLS-DA performed well in identifying the defect-free samples from the samples with defects, the classification accuracy was of 98.33% and 96.67% for calibration set and prediction set, respectively.
4. Moreover, further studies are still needed to cover more types of defects on the surface of solid wood boards. Also, a more robust discrimination model for different kinds of wood is desired.

ACKNOWLEDGMENTS

The authors are grateful for the support of the National Forestry Bureau of the 948 Project (Grant No. 2015-4-52) and the support of the Fundamental Research Funds for the Central Universities (Grant No. 2572015AB14).

REFERENCES CITED

Baradit, E., Aedo, R., and Correa, J. (2006). "Knots detection in wood using microwaves," *Journal of Wood Science and Technology* 40(2), 118-123. DOI: 10.1007/s00226-005-0027-8

Cristhian, A. C., Sanchez, R., and Baradit, E. (2008). "Detection of knots using X-ray tomographies and deformable contours with simulated annealing," *Wood Research* 53(2), 57-66.

Danvind, J. (2002) "PLS prediction as a tool for modeling wood properties," *Holz als Roh-und Werkstoff* 60(2), 130-140. DOI: 10.1007/s00107-001-0271-z

Eom, C. D., Park, J. H., Choi, I. G., Choi, J. W., Han, Y., and Yeo, H. (2013). "Determining surface emission coefficient of wood using theoretical methods and near-infrared spectroscopy," *Wood and Fiber Science* 45(1), 76-83.

Kabir, M. F., Schmoldt, D. L., Araman, P. A., Schafer, M. E., and Lee, S. M. (2003). "Classifying defects in pallet stringers by ultrasonic scanning," *Wood and Fiber Science* 35(3), 341-350.

Ken, W., Isao, K., Shuetsu, S., Naohiro, K., and Shuichi, N. (2013). "Nondestructive evaluation of drying stress level on wood surface using near-infrared spectroscopy," *Journal of Wood Science and Technology* 47(2), 299-315. DOI: 10.1007/s00226-012-0492-9

Li, X. L., Yi, S. L., He, S. L., Lv, Q., Xie, R. J., Zheng, Y. Q., and Deng, L. (2016). "Identification of pummelo cultivars by using Vis/NIR spectra and pattern recognition methods," *Precision Agriculture* 17(3), 365-374. DOI: 10.1007/s11119-015-9426-5

Nascimbem, L. B. L. R., Rubini, B. R., and Poppi, R. J. (2013). "Determination of quality parameters in moist wood chips by near infrared spectroscopy combining PLS-DA and support vector machines," *Journal of Wood Chemistry and Technology* 33(4), 247-257. DOI: 10.1080/02773813.2013.783075

Rinnan, A., van den Berg, F., and Engelsen, S. B. (2009). "Review of the most common pre-processing techniques for near-infrared spectra," *Trac-trends in Analytical Chemistry* 28(10), 1201-1222. DOI: 10.1016/j.trac.2009.07.007

Santos, A., Alves, A., Simoes, R., Pereira, H., Rodrigues, J., and Schwanninger, M. (2012). "Estimation of wood basic density of *Acacia melanoxylon* (R. Br.) by near infrared spectroscopy," *Journal of Near Infrared Spectroscopy* 20(2), 267-274. DOI: 10.1255/jnirs.386

Suykens, J. A. K., Gestel, T. V., Brabanter, J. D., Moor, B., and Vandewalle, J. (2002). *Least Squares Support Vector Machines*, World Scientific, Singapore.

Takizawa, K., Nakano, K., Ohashi, S., Yoshizawa, H., Wang, J., and Sasaki, Y. (2014). "Development of nondestructive technique for detecting internal defects in Japanese radishes," *Journal of Food Engineering* 126, 43-47. DOI: 10.1016/j.jfoodeng.2013.10.041

Todorović, N., Popović, Z., and Milić, G. (2015). "Estimation of quality of thermally modified beech wood with red heartwood by FT-NIR spectroscopy," *Journal of Wood Science and Technology* 49(3), 527-549. DOI: 10.1007/s00226-015-0710-3

Yang, Z., Lv, B., and Fu, Y. J. (2012). "The relationship between near infrared spectroscopy and surface color of eight rosewoods," *Advanced Materials Research* 479-481, 1772-1776. DOI: 10.4028/www.scientific.net/AMR.479-481.1772

Yang, Z., Zhang, M. M., Li, K., and Chen, L. (2016). "Rapid detection of knot defects on wood surface by near infrared spectroscopy coupled with partial least squares discriminant analysis," *BioResources* 11(1), 2557-2567. DOI: 10.15376/biores.11.1.2557-2567

Zhang, M. M., Liu, Y. N., and Yang, Z. (2015). "Correlation of near infrared spectroscopy measurements with the surface roughness of wood," *BioResources* 10(4), 8505-8517. DOI: 10.15376/biores.10.4.8505-8517

Zhu, X. H., Fang, L. J., Gu, J. S., and Guo, W. C. (2016). "Feasibility investigation on determining soluble solids content of peaches using dielectric," *Food Analytical Methods* 9(6), 1789-1798. DOI: 10.1007/s12161-015-0348-7

Article submitted: September 4, 2016; Peer review completed: October 22, 2016; Revised version received and accepted: October 27, 2016; Published: November 2, 2016.
DOI: 10.15376/biores.12.1.19-28